Molecular Electronics Hot Paper

International Edition: DOI: 10.1002/anie.201903898
German Edition: DOI: 10.1002/ange.201903898

Anisotropic Conductivity at the Single-Molecule Scale

*Sepideh Afsari, Parisa Yasini, Haowei Peng, John P. Perdew, and Eric Borguet**

Abstract: *In most junctions built by wiring a single molecule between two electrodes, the electrons flow along only one axis: between the two anchoring groups. However, molecules can be anisotropic, and an orientation-dependent conductance is expected. Here, we fabricated single-molecule junctions by using the electrode potential to control the molecular orientation and access individual elements of the conductivity tensor. We measured the conductance in two directions, along the molecular plane as the benzene ring bridges two electrodes using anchoring groups (upright) and orthogonal to the molecular plane with the molecule lying flat on the substrate (planar). The perpendicular (planar) conductance is about 400 times higher than that along the molecular plane (upright). This offers a new method for designing a reversible room-temperature single-molecule electromechanical switch that controllably employs the electrode potential to orient the molecule in the junction in either "ON" or "OFF" conductance states.*

Introduction

The ultimate goal in the development of nano-electronics is controllable charge transport through molecules that operate as electronic components[1] such as rectifiers[2] and switches.[3] In studying molecular conductance at the single-molecule level, junctions are typically fabricated by wiring a single molecule between two metal electrodes via anchoring groups[4,5] such as thiols[6] and amines[7] that provide sufficient electronic coupling between the metal and the molecule. The contact between the single molecule and the electrodes must be robust, reproducible, and able to provide a strong coupling between the molecule and the electrodes so that the junction is stable and has a low contact resistance.[8] In such conventional single molecule conductivity (SMC) measurements, charge transport is measured along one axis, that is, between two anchoring groups.[8,9] Our previous study in measuring charge transport perpendicular to the aromatic ring of a benzene derivative for the first time revealed that the junctions formed by direct contact between the gold electrodes and the π-system of the benzene ring of the molecule result in a molecular conductance that is two orders of magnitude higher than the conductance of a benzene ring connected via standard anchoring groups.[10] Furthermore, DFT calculations showed that the conductance perpendicular to the[11] ring is about 0.1 G_o.[12–14] ($G_o = 2e^2/h$ where e is the electron charge and h is Planck's constant[4]) while the conductance of single-benzene-derivative junctions formed with standard linker groups is about 0.005–0.01 G_o.[15]

These observations led us to the hypothesis that for some benzene derivatives, there could be an orientation-dependent conductance in the junction. Thus, the conductance of single-molecule junctions is anisotropic because of the different possible contact geometries, that is, electrode-anchoring groups (upright) versus direct electrode–π contact (planar), and likely associated with very different conductance values. As any structural transformation of single-molecule junctions triggered by an external chemical or physical stimulus (e.g., applied force,[16] light,[17] tunneling current,[18] redox reactions,[11,19] or a change in pH[20]) that results in altered electronic properties of the molecular junction can be utilized in designing single-molecule electronic switches,[21] we propose employing this strategy to design an electromechanical single-molecule switch. We show that we can controllably alternate the single-molecule switch between high or "ON" and low or "OFF" conductance modes by employing electrode potential as an external stimulus that induces a transition in the single-molecule orientation in the junction from "planar" to "upright" (Scheme 1 a).

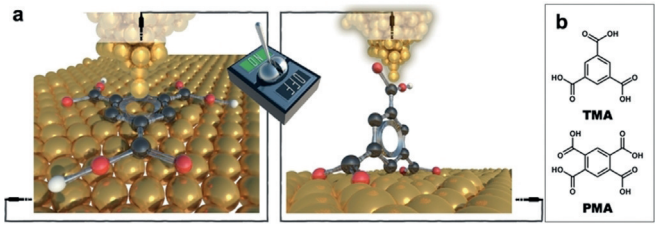

Scheme 1. a) The two possible junction configurations formed by direct interaction of the Au electrodes to either the aromatic ring or the carboxylic acid groups of single TMA molecules. b) Molecular structure of the benzenecarboxylic acids used in this study.

Results and Discussion

Two benzenecarboxylic acids, namely trimesic acid (TMA) and pyromellitic acid (PMA) containing three and four peripheral carboxylic groups (COOH), respectively (Scheme 1 b), are used in this study to build molecular junctions. We reproducibly fabricate orientation-controlled single-molecule junctions by utilizing a combination of

[*] Dr. S. Afsari, P. Yasini, Dr. J. P. Perdew, Dr. E. Borguet
Department of Chemistry, Temple University
1901 N. 13th St., Philadelphia, PA 19122 (USA)
E-mail: eborguet@temple.edu
Dr. H. Peng, Dr. J. P. Perdew
Department of Physics, Temple University
1925 N 12th St., Philadelphia, PA 19122 (USA)
Supporting information and the ORCID identification number(s) for the author(s) of this article can be found under: https://doi.org/10.1002/anie.201903898.

electrochemical scanning tunneling microscopy (EC-STM) break junction (EC-STM-BJ) and high-resolution STM imaging under electrode potential control (see the Supporting Information). The potential of the gold electrode surface (working electrode) is employed to control the orientation of the single molecule in the junction between the gold tip and the electrode surface while the conductivity of the single molecule is measured for each orientation. The anisotropic conductivity of single-molecule junctions in two orientations (upright and planar) of the central benzene rings (Scheme 1 a) is investigated. TMA molecules (Scheme 1 b) are adsorbed in planar geometry at a negatively charged Au surface with the benzene ring oriented parallel to the surface.[22] We show that junctions formed with a planar orientation have a conductance that is about one tenth of the conductance quantum, G_o. This conductance is significantly higher than that achieved with an upright orientation of TMA molecules in the junction and also more than two orders of magnitude higher than the conductance of single-molecule junctions of benzene derivatives formed with conventional linkers such as thiols and amines.[15] The high conductance that we observe suggests strongly that direct coupling between the π-system of the benzene ring and the gold STM tip results in charge transport perpendicular to the benzene ring. This hypothesis is well supported by density functional theory (DFT) calculations in this study for TMA, with the calculated conductance being about 300 times higher for the planar than for the upright orientation. Hence, the electrode potential can, in principle, be employed as an external stimulus to switch the orientation of a single molecule in an electrical junction inducing ON or OFF conductance states of a single-molecule switch.

As the first step in fabricating the proposed electromechanical single-molecule switch, we conducted EC-STM imaging to clarify the molecule orientation on the charged Au surface. The potential of zero charge, where the surface charge is zero, for the electrochemically reconstructed Au-(111)–$(22 \times \sqrt{3})$ and the Au(111)–(1×1) surfaces are 270 mV and 230 mV versus the saturated calomel electrode (SCE), respectively.[23] STM images of the electrified Au(111) electrode in the presence of TMA in sulfuric acid show that TMA molecules (Scheme 1 b) are physisorbed at negative potentials (or negative surface charge densities) with the benzene ring lying flat on the gold electrode surface, forming long range ordered structures because of intermolecular hydrogen bonds between COOH groups (Figure 1 a). Moving to positive potentials (positive surface charge densities), TMA molecules are chemisorbed with the ring oriented upright because of the deprotonation of COOH groups,[24] which coordinate to the gold electrode (Figure 1 d; STM image analysis can be found in the Supporting Information, Figure S2).

Following the STM imaging, SMC measurements were conducted to form planar TMA single-molecule junctions by repeatedly bringing the STM tip into contact with the

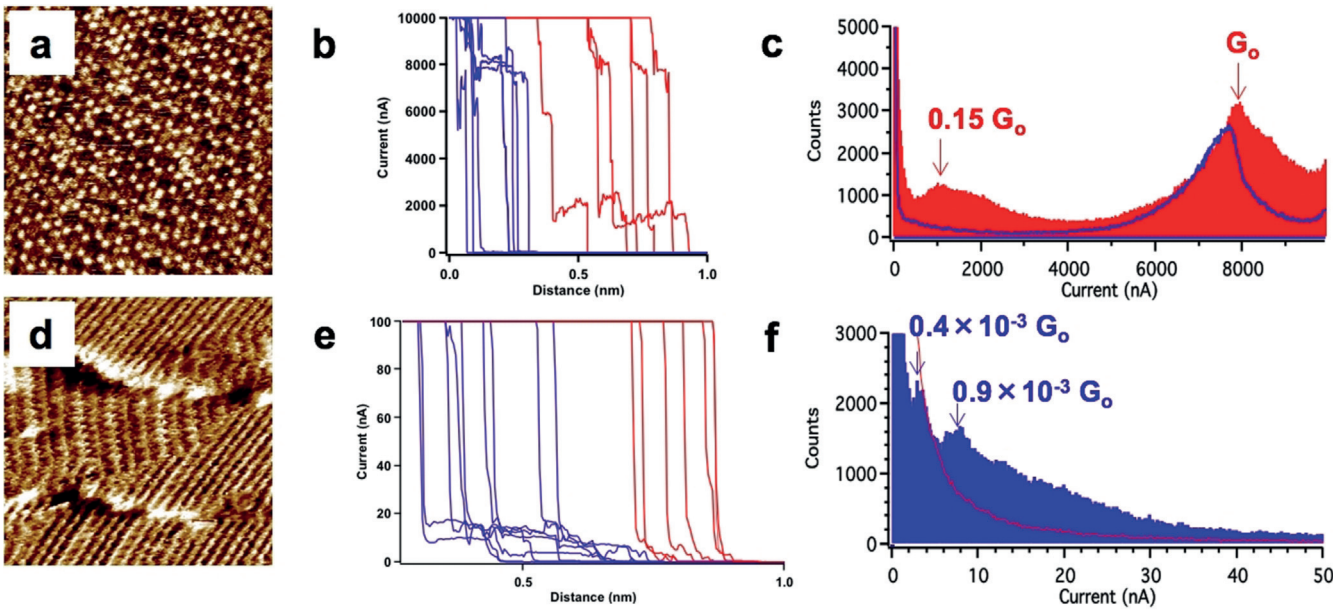

Figure 1. STM imaging and conductance measurements of trimesic acid (TMA). a) 20×20 nm^2 EC-STM image of TMA on a negatively charged ($E_{surface} = -0.10$ V_{SCE}) Au(111) electrode indicating benzene rings parallel to the surface. b) Examples of individual current–distance traces at high current regions collected on the negatively (red) and the positively (blue) charged Au(111) surfaces. c) All-data point EC-STM-BJ current histograms of TMA at high current regions collected on a negatively charged ($E_{surface} = -0.10$ V_{SCE}) Au(111) electrode without any data selection of 9070 individual current–distance traces (red) and on a positively charged ($E_{surface} = +0.75$ V_{SCE}) Au(111) electrode without any data selection of 7609 individual current–distance traces (blue). d) 10×10 nm^2 EC-STM image of TMA on a positively charged Au(111) electrode ($E_{surface} = +0.75$ V_{SCE}) showing an ordered structure of TMA molecules standing upright. e) Example of individual current–distance traces collected on the negatively (red) and the positively (blue) charged Au(111) surfaces. f) All-data point EC-STM-BJ current histograms of TMA at low current regions collected on a positively charged Au(111) electrode ($E_{surface} = +0.75$ V_{SCE}) without any data selection of 2974 individual current–distance traces (blue) and a negatively charged Au(111) electrode ($E_{surface} = -0.10$ V_{SCE}) without any data selection of 2970 individual current–distance traces (blue).

electrified Au(111) electrode in the presence of the TMA monolayer while current–distance traces were recorded in the 1–10000 nA current range. Displacement of the STM tip away from the negatively charged Au(111) surface ($E_{surface} = -0.1\ V_{SCE}$) in the presence of the TMA monolayer gave rise to quasi-exponentially decaying traces that are interrupted by current plateaus (or steps) interpreted as resulting from molecular junction formation, allowing the current to remain approximately constant even as the distance between tip and substrate increases (Figure 1b, red traces). A statistical assessment of repeated EC-STM-BJ measurements is provided by conductance histograms, generated without any data selection from over 10000 measurements, that show a clear peak at a conductance value of 0.15 G_o for negative potentials (Figure 1c, red). At positive potentials, only quasi-exponentially decaying traces without any plateaus or steps are observed, suggesting the absence of flat-lying molecules bridging the electrode potential towards positive values (Figure 1b, blue traces). Thus, the conductance peak observed at 0.15 G_o disappears upon changing the electrode potential towards positive values (Figure 1c, blue).

As a control, and in order to confirm that the observed conductance peak corresponds to single TMA molecules, we measured the conductance in the absence of the TMA monolayer (Figure 2d). These histograms are generated without any data selection from over 2000 current–distance measurements on Au(111) in air, in sulfuric acid (without TMA) at negative potentials, and with 1 mM TMA in sulfuric acid without electrode potential control (details of the SMC experiments can be found in the Supporting Information, Figure S1d). In none of these control STM-BJ measurements, which are all characterized by the absence of the ordered TMA monolayer, do we see a peak corresponding to charge transport through molecular junctions (Figure 2d), confirming that the 0.15 G_o peak represents the conductance of single-molecule junctions formed with the flat-lying TMA molecules in the assembled monolayer. Additionally, to confirm the bias potential dependence, we investigate the current–bias relationship for this conductance feature by varying the bias voltage (E_{bias}) from −0.10 V to −0.05 V in SMC experiments while the $E_{surface} = -0.1\ V_{SCE}$ is maintained to give a negatively charged surface (Supporting Information, Figure S3). The current peak in the histogram (Figure S3B) moves to lower currents proportionally to E_{bias} in accordance with Ohm's law ($V = IR$), and the resulting conductance is constant.

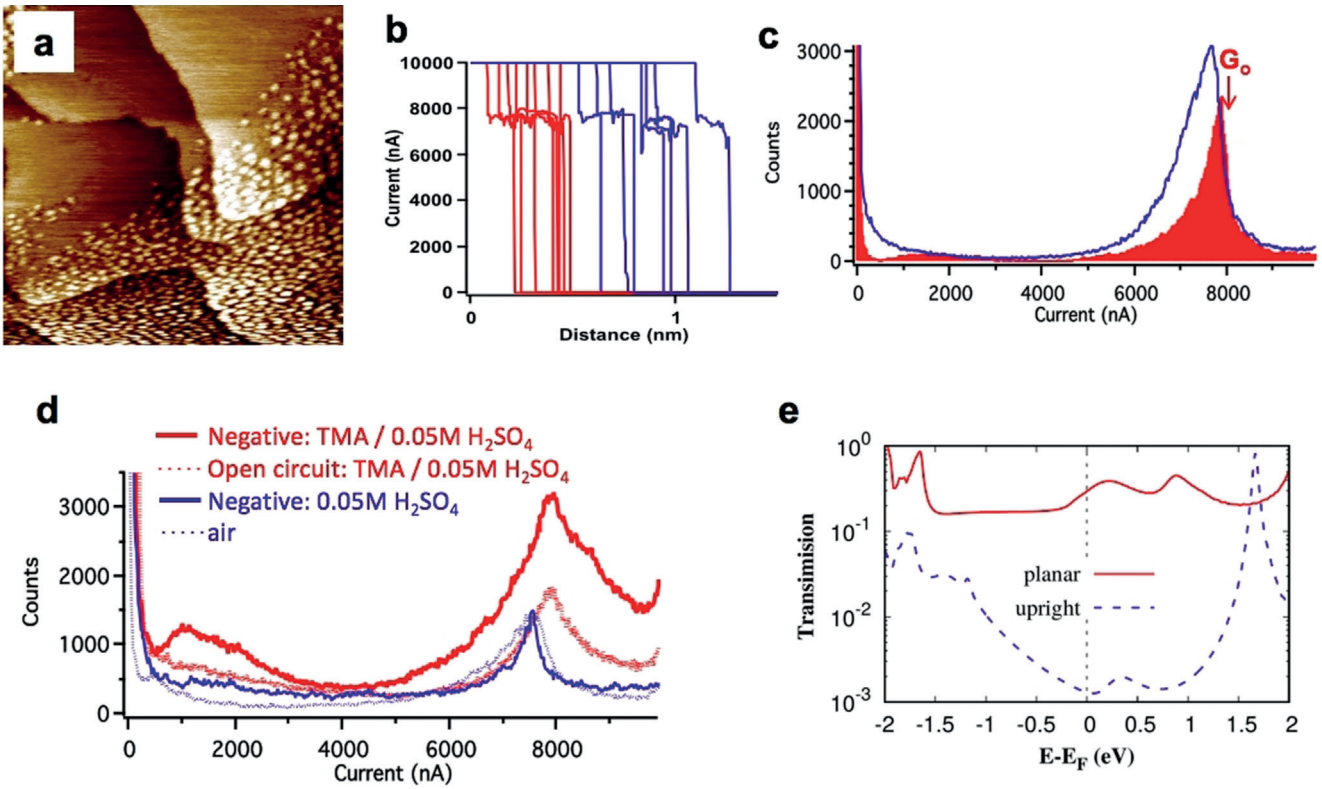

Figure 2. Control STM imaging and conductance measurements and DFT calculations. a) 100×100 nm² EC-STM image of pyromellitic acid (PMA) on a negatively charged ($E_{surface} = -0.10\ V_{SCE}$) Au(111) surface. b) Example of individual current–distance traces collected in the presence of pyromellitic acid (PMA) on the negatively (red) and the positively (blue) charged Au(111) surfaces. c) EC-STM-BJ current histograms of PMA on negatively (red) and positively (blue) charged Au(111) electrodes without any data selection of 5029 and 3071 individual current–distance traces, respectively. d) STM-BJ current histograms without any data selection of: solid red line: TMA in 0.05 M H_2SO_4 on a negatively charged Au(111) surface ($E_{surface} = -0.10\ V_{SCE}$ and $E_{bias} = -0.10$ V); dotted red line: TMA in 0.05 M H_2SO_4 and no electrode potential control on Au(111) ($E_{bias} = -0.10$ V); solid blue line: 0.05 M H_2SO_4 without TMA on a negatively charged Au(111) surface ($E_{surface} = -0.10\ V_{SCE}$ and $E_{bias} = -0.10$ V; dotted blue line: Au(111) in air ($E_{bias} = -0.10$ V). e) The transmission spectra for TMA single-molecule junctions between the Au(111) surface and the STM tip for both the planar and the upright TMA orientations.

In our STM-BJ measurements, because the maximum current typically only allows the detection of the conductance quantum, G_o (ca. 77500 nA at $E_{bias} = 100$ mV), the contact is insufficient to make more than a single Au atom junction. Therefore, we conclude that neither the tip nor the overall monolayer is destroyed.[10] We attribute the 0.15 G_o conductance peak to charge transport perpendicular to the benzene ring (Scheme 1a). Intermolecular hydrogen bonding between neighboring molecules immobilizes TMA molecules on the Au(111) surface, allowing direct contact between the Au electrodes and the π-system of the benzene ring. In these junctions, the benzene ring is planar on the gold substrate and thus charge transport between the electrodes occurs perpendicular to that plane.

Next, we investigated the "OFF" conductance state of the TMA single-molecule switch under positive potentials and in much lower current regions (1–100 nA). Changing the gold electrode potential to positive values drives the molecular orientation from planar to upright (Figure 1d) due to the deprotonation of the carboxylic acid groups.[24] Ordered structures of TMA molecules are formed by pairs of upright and parallel-aligned TMA molecules coordinated to the positively charged substrate surface through one deprotonated carboxylate (COO^-) group and possible formation of intermolecular hydrogen bonds involving the solution-directed carboxyl groups (COOH).[25] In this arrangement, the parallel phenyl rings of one dimer are separated by 0.35 nm (Supporting Information, Figure S2C,D). The single-molecule junctions on a positively charged Au(111) surface ($E_{surface} = +0.75\ V_{SCE}$) are expected to be formed with contacts between carboxylic acid groups and gold electrodes (Scheme 1a) leading to a current plateau or step in the current–distance traces (Figure 1e, blue traces) in the low current regions. Thus, the 0.15 G_o (high) conductance peak disappears and two (low) conductance peaks at about $0.4 \times 10^{-3}\ G_o$ and $0.9 \times 10^{-3}\ G_o$ are present in the histograms (Figure 1f, blue). When measuring the conductance of the single molecules at the junction, it is possible that molecules deviate from the idealized, perfectly planar or upright geometries. However, the lengths of the molecular junctions in the current–distance traces shown in Figure 1b,e are consistent with flat-oriented and upright molecules, respectively. Furthermore, when the molecules deviate from the ideal configurations, charge transport through such geometries should result in the broadening of the conductance peak in the current histogram.

Previously reported conductance values of single-molecule junctions formed with 1,4-benzenedithiol range from 0.01 G_o to $4 \times 10^{-4}\ G_o$.[15,26–28] This leads us to attribute the $0.4 \times 10^{-3}\ G_o$ peak to the conductance of single TMA molecules bridging the electrodes through the carboxylic acid groups while we suggest that the $0.9 \times 10^{-3}\ G_o$ peak is the collective conductance due to the simultaneous contact between two (pairs of upright and parallel-aligned) TMA molecules and the STM tip. Neither of these conductance peaks was observed in histograms acquired at negative potentials in the low current region (Figure 1f, red). We believe that the hydrogen bonding between neighboring TMA molecules at the negatively charged surface is strong enough to keep the molecules parallel to the surface. Thus, junctions with direct contact between the carboxylic acid groups and the gold electrodes cannot easily be formed at negative potentials, leading to current–distance traces without any current plateau or step in the low current region (Figure 1e, red traces).

To confirm that the observed peaks at $0.4 \times 10^{-3}\ G_o$ and $0.9 \times 10^{-3}\ G_o$ actually represent the signature of molecular conductance, we investigated the current–bias relationship for these conductance features by varying the bias voltage (E_{bias}) from −0.10 V to −0.30 V in SMC experiments while the potential of the surface ($E_{surface}$) is maintained at $+0.75\ V_{SCE}$ (Supporting Information, Figure S4). The current maxima in the histograms increase proportionally to E_{bias} revealing a constant conductance (Figure S4B). The bias independence of the conductance indicates the molecular nature of the conductance peaks attributed to transport through the benzene ring of the upright TMA molecule in the junction with carboxylic acid groups as linkers.

To further test the hypothesis that a planar geometry stabilized by long-range-ordered structures is necessary to observe the high conductance state, we measured transport through pyromellitic acid (PMA), which by design and because of the hindrance of the four carboxylic acid groups (Scheme 1b) appears unlikely to form long-range ordered structures with a planar geometry of benzene rings on the gold substrate.[29] Thus, a direct Au–π contact should rarely form because the molecule is unlikely to be oriented with its benzene ring perpendicular to the junction axis.

Our STM images of PMA do not reveal any ordered structure (Figure 2a). Instead, the surface is covered with bright features varying in size from one to several nanometers that can be tentatively assigned to clusters of a few PMA molecules agglomerated because of hydrogen bonding between the carboxylic acid groups (Figure 2a). The conductance histograms of PMA collected with negative and positive potentials are similar. Notably, the dominant 0.15 G_o peak is missing in both histograms (Figure 2c, red and blue). Instead, a few broad peaks are present (Figure 2c, red) quite unlike the feature for TMA.

To confirm that the peaks that we observe in the PMA histogram are not dominant enough to be attributed to a molecular conductance of a specific geometry, we can compare the amplitude of the peaks in the region of 0–2000 nA with the height of the G_o peak. In the TMA histograms collected with the same experimental setup (negatively charged Au(111) surface), the peak in the region of 0–2000 nA is clear with a height of about one fourth of the G_o peak (Figure 1c) while in the PMA histogram, the minor peaks are at most one tenth of the G_o peak (Figure 2c). We also conducted SMC experiments for PMA in the low current region (1–100 nA), and we did not see any peak corresponding to charge transport through junctions formed via carboxylic linkers (Supporting Information, Figure S5). These control measurements show that in the case of PMA, where no long-range order was observed, single-molecule junctions with the benzene ring perpendicular to the Au STM tip are not formed.

To further elucidate that such an ON/OFF switching does not arise from some uncertainty related to the atomic-level details within our experimental setting, we performed DFT calculations with SIESTA[30] and TranSIESTA.[31] We used the Troullier–Martins norm-conservation pseudopotentials,[32] the so-called SZP pseudo-atomic orbital (PAO) basis for Au, the DZP basis for other elements, and the consistent-exchange van der Waals density functional (vdW-DF-cx)[33] for the exchange correlation approximation. The computation procedure is available in the Supporting Information, Section S6. For the planar orientation, the benzene ring takes the hcp-A configuration,[34] and for the upright orientation, the deprotonated COOH groups directly bond to Au atoms of the Au(111) substrate as in the experiment. The transmission spectrum from non-equilibrium Green's functional computation is shown in Figure 2e, where the transmission at the Fermi level is an excellent estimator for low-bias conductance. Thanks to some error cancellation, the DFT results, 0.3 and 0.001 G_o for the planar and upright orientations, respectively, agree quite well with the experimental values. More importantly, the DFT computation confirms that such strong orientation dependence is intrinsic.

Based on these observations and calculations, we conclude that we have controllably measured charge transport/conductance along two different axes: one with the benzene ring lying flat on the substrate perpendicular to the STM tip (planar) and the other one with the molecule bridging between the two electrodes using carboxylic acids as anchoring groups (upright). The junctions with planar molecular orientation have a conductance that is significantly higher (by a factor of 400) than junctions with molecules in an upright geometry.

Conclusion

Employing an electrochemical STM setup has enabled us to control the orientation of single molecules between two gold electrodes and, for the first time, measure the conductance in a controlled manner along two different axes. We developed a strategy to use the potential of the gold (working) electrode to controllably change the orientation of benzenecarboxylic acids in the junction from planar to upright and to measure the conductance of single molecules either perpendicular to or along the benzene ring. The measured conductance of TMA molecules in these two distinct orientations determined the two conductance states of the single molecule in the junction. Hence, we introduce a new class of single-molecule junctions that exhibit well-defined orientation-dependent anisotropic conductivity. Furthermore, the junctions with the planar molecular orientation have a conductance significantly higher (by a factor of ca. 400) than that of junctions with molecules in the upright geometry. Thus, we can use the electrode potential as a knob to design a single-molecule electromechanical switch with high ON/OFF conductance ratios. We suggested that this phenomenon is applicable in designing single-molecule switches where the orientation of the molecules in the junctions is controlled utilizing the electrode potential as a knob. This offers a new method for designing a robust, room-temperature electromechanical single molecule switches with high "ON" to "OFF" conductance ratios.

Acknowledgements

We acknowledge funding for this work from the National Science Foundation (CHE-1508567) and as part of the Center for Complex Materials from First Principles, an Energy Research Center funded by the U.S. Department of Energy, Office of Science, Basic Energy Sciences, under Grant No. DE-SC0012575.

Conflict of interest

The authors declare no conflict of interest.

Keywords: molecular electronics · molecular switches · single-molecule studies · scanning tunneling microscopy

How to cite: *Angew. Chem. Int. Ed.* **2019**, *58*, 14275 – 14280
Angew. Chem. **2019**, *131*, 14413 – 14418

[1] A. H. Flood, J. F. Stoddart, D. W. Steuerman, J. R. Health, *Science* **2004**, *306*, 2055 – 2056.
[2] A. Aviram, M. A. Ratner, *Chem. Phys. Lett.* **1974**, *29*, 277 – 283.
[3] M. del Valle, R. Gutierrez, C. Tejedor, G. Cuniberti, *Nat. Nanotechnol.* **2007**, *2*, 176 – 179.
[4] B. Xu, N. J. Tao, *Science* **2003**, *301*, 1221 – 1223.
[5] Z. Li, M. Smeu, M. A. Ratner, E. Borguet, *J. Phys. Chem. C* **2013**, *117*, 14890 – 14898.
[6] X. Li, J. He, J. Hihath, B. Xu, S. M. Lindsay, N. Tao, *J. Am. Chem. Soc.* **2006**, *128*, 2135 – 2141.
[7] F. Chen, X. Li, J. Hihath, Z. Huang, N. Tao, *J. Am. Chem. Soc.* **2006**, *128*, 15874 – 15881.
[8] N. J. Tao, *Nat. Nanotechnol.* **2006**, *1*, 173 – 181.
[9] A. Nitzan, M. A. Ratner, *Science* **2003**, *300*, 1384 – 1390.
[10] S. Afsari, Z. Li, E. Borguet, *Angew. Chem. Int. Ed.* **2014**, *53*, 9771 – 9774; *Angew. Chem.* **2014**, *126*, 9929 – 9932.
[11] Z. Li, H. Li, S. Chen, T. Froehlich, C. Yi, C. Schönenberger, M. Calame, S. Decurtins, S. X. Liu, E. Borguet, *J. Am. Chem. Soc.* **2014**, *136*, 8867 – 8870.
[12] M. Mine, T. Tsutsui, E. Miyoshi, *Jpn. J. Appl. Phys.* **2008**, *47*, 8033 – 8038.
[13] H. Wang, Z. Jiang, Y. Wang, S. Sanvito, S. Hou, *ChemPhysChem* **2016**, *17*, 2272 – 2277.
[14] Y. Komoto, S. Fujii, T. Nishino, M. Kiguchi, *Beilstein J. Nanotechnol.* **2015**, *6*, 2431 – 2437.
[15] M. Kiguchi, H. Nakamura, Y. Takahashi, T. Takahashi, T. Ohto, *J. Phys. Chem. C* **2010**, *114*, 22254 – 22261.
[16] J. N. Ladenthin, T. Frederiksen, M. Persson, J. C. Sharp, S. Gawinkowski, J. Waluk, T. Kumagai, *Nat. Chem.* **2016**, *8*, 935 – 940.
[17] C. Jia et al., *Science* **2016**, *352*, 1443 – 1446.
[18] B. E. Tebikachew, H. B. Li, A. Pirrotta, K. Börjesson, G. C. Solomon, J. Hihath, K. Moth-Poulsen, *J. Phys. Chem. C* **2017**, *121*, 7094 – 7100.
[19] L. J. O'Driscoll, J. M. Hamill, I. Grace, B. W. Nielsen, E. Almutib, Y. Fu, W. Hong, C. J. Lambert, J. O. Jeppesen, *Chem. Sci.* **2017**, *8*, 6123 – 6130.

[20] Z. Li, M. Smeu, S. Afsari, Y. Xing, M. A. Ratner, E. Borguet, *Angew. Chem. Int. Ed.* **2014**, *53*, 1098 – 1102; *Angew. Chem.* **2014**, *126*, 1116 – 1120.
[21] C. D. Frisbie, *Science* **2016**, *352*, 1394 – 1395.
[22] Z. Li, B. Han, L. J. Wan, T. Wandlowski, *Langmuir* **2005**, *21*, 6915 – 6928.
[23] S. Wu, J. Lipkowski, O. M. Magnussen, B. M. Ocko, T. Wandlowski, *J. Electroanal. Chem.* **1998**, *446*, 67 – 77.
[24] B. Han, Z. Li, S. Pronkin, T. Wandlowski, *Can. J. Chem.* **2004**, *82*, 1481 – 1494.
[25] B. Han, Z. Li, T. Wandlowski, *Anal. Bioanal. Chem.* **2007**, *388*, 121 – 129.
[26] X. Xiao, B. Xu, N. Tao, *J. Am. Chem. Soc.* **2004**, *126*, 5370 – 5371.
[27] M. A. Reed, *Science* **1997**, *278*, 252 – 254.
[28] J. Ulrich, D. Esrail, W. Pontius, L. Venkataraman, D. Millar, L. H. Doerrer, *J. Phys. Chem. B* **2006**, *110*, 2462 – 2466.
[29] M. Lackinger, S. Griessl, T. Markert, F. Jamitzky, W. M. Heckl, *J. Phys. Chem. B* **2004**, *108*, 13652 – 13655.
[30] M. Soler, E. Artacho, J. D. Gale, A. Garc, J. Junquera, P. Ordej, S. Daniel, *J. Phys. Condens. Matter* **2002**, *11*, 2745.
[31] N. Papior, N. Lorente, T. Frederiksen, A. García, *Comput. Phys. Commun.* **2017**, *212*, 8 – 24.
[32] N. Troullier, J. L. Martins, *Phys. Rev. B* **1991**, *43*, 8861 – 8869.
[33] K. Berland, P. Hyldgaard, *Phys. Rev. B* **2014**, *89*, 035412.
[34] H. Peng, Z. Yang, J. P. Perdew, J. Sun, *Phys. Rev. X* **2016**, *6*, 041005.

Manuscript received: March 30, 2019
Accepted manuscript online: June 25, 2019
Version of record online: August 7, 2019

